Ultrasonic characterization of ultra-thin elastic layer using retrieve function *

QIAN Ming WAN Mingxi
(*Biomedical Engineering Dept., Xi'an Jiaotong University* Xi'an 710049)
CAO Wenwu
(*Intercollege Materials Research Lab., Pennsylvania State University* PA 16802 U.S.A)

Received Aug. 27, 1997
Revised Sept. 19, 1997

Abstract Using frequency domain retrieve function, a method is presented for characterizing ultra-thin plate by low frequency ultrasound. "Ultra-thin" means that the thickness of specimen is much less than the wavelength. The through-transmission retrieve function is examined in detail. In conjunction with the method of least squares, the amplitude spectrum, phase spectrum and complex spectrum are all used to determine the best estimation. An analysis of some typical sources of the estimate deviation is presented. The sensitivities of the retrieve function to acoustical parameters and its significance in the propagation of errors have been derived and well discussed. In experimental study the technique is employed to characterize the brass sheets ranging from 25.4 μm to 152.4 μm with a broadband 2 MHz transducer. It is observed that the agreement between the nominal value and the estimation is excellent.
PACS numbers: 43.35, 43.60.

1 Introduction

There are various situations of technological importance in which one wishes to carry out a non-destructive evaluation (NDE) of the acoustic properties (thickness, wave-speed, attenuation and density) of thin elastic layers, such as characterizing the quality of welding seam, the strength of adhesive bonding layers, layers in composite structures, and thin films on substrate. Over the past thirty years, ultrasonic determination of the acoustical properties has received considerable attention and a number of techniques have been developed. Among these are time-of-flight method[1-2], pulse-echo method[1-3], pulse interference[4] and resonance testing method[5-6] *et al.* However, in order to use any of these methods, it is required that two successful echoes (and therefore, all subsequent echoes) from the specimen can be separated in time domain. In other words, the duration time of incident pulse should be less than the round-trip

* This work was supported in part by Office of Naval Research, U. S. A, under grant #N00014-93-1-0340 and in part by Trans-century Training Program for Talents from Chinese Government grants (1994)

time in specimen or the specimen thickness should exceed half of the pulse length. Therefore, using aforementioned methods, as specimen thickness, h, decreases, the frequency of the ultrasonic wave used must be increased. For example, if h is on the order of 10 μm, the frequency would have to be higher than 150 MHz[3]. The use of such high frequencies not only greatly increases the cost for the specified transducer and associated broadband instrumentation, but also limits its application because of the very short penetration depth. It is well known that at high frequencies strong attenuation occurs due to the increase of scattering centers.

Recently, some so-called non-separable pulse methods[6-14] have been developed for the ultrasonic NDE of sub-wavelength elastic layers with using low frequency ultrasound. Kinra *et al.* firstly introduced thickness-to-wavelength ratio (h/λ) to quantify the relative thickness of a specimen. Correspondingly, the attainable minimum h/λ ratio is a key criteria to assess the performance of each method for characterizing the thin plate. The minimum thickness which can be successfully measured using conventional methods is approximately 2.5λ-3λ, however, the non-separable pulse methods are suitable for sub-wavelength samples. Especially, some recently presented techniques, such as the frequency-domain transfer function method[6-8], time-domain direct measurement method[9] and time-domain least squares method[10-12], have been successfully applied to measure thin layers on the order of $10^{-2}\lambda(h/\lambda < 0.1)$. Currently, there are two main branches in ultrasonic NDE of thin layers, one is multi-layered specimen characterizing[15-18] which is motivated by the immense engineering need for NDE of the composite, adhesive, welding and coating materials, the other is keeping attention on developing a more broad-based technique that can provide better performance in characterization.

In this paper, a frequency-domain retrieve function method has been presented for characterizing an ultra-thin plate. By "ultra-thin", we mean the thickness of specimen is much less than the wavelength. In conjunction with the least squares method, the amplitude spectrum, phase spectrum and complex spectrum of the through-transmission retrieve function are all used to determine the best estimation. An analysis of some typical sources affecting estimate precision is presented. The sensitivity of the retrieve function to acoustical parameters and its significance in the propagation of errors have been derived and well discussed. In experimental study the technique is employed to characterize the brass sheets ranging from 25.4 μm to 152.4 μm with a broadband 2 MHz transducer. It is observed that the agreement between the nominal value and the estimation is excellent.

2 Numerical analysis procedures

2.1 Retrieve function

Consider an elastic layer immersed in fluid (water). A Langrangian space-time location diagram of the wavefront traveling through the layer is shown in Fig. 1. A plane finite-duration incident pulse, $f(t)$, (ray 1 in Fig. 1) is normally incident on the plate. This results in a series of reflected pulses (rays 2, 6, 10 ...) and transmitted pulses (rays 4, 8, 12 ...). As the specimen thickness decreases the time interval between two successive echoes decreases and finally the pulses cannot be separated in time domain. The typical incident and transmitted signals are

shown in Fig. 2. It can be shown that the specimen signal, $g(t)$, (total transmitted field) may be written as[10]

$$g(t) = T_{01}T_{10}\sum_{m=0}^{\infty} R_{10}^{2m} f(t - h[(2m+1)s - s_0]) \tag{1}$$

where $R_{ij} = (Z_i - Z_j)/(Z_i + Z_j)$ and $T_{ij} = 2Z_i/(Z_i + Z_j)$ are, respectively, the reflection and transmission coefficients, the subscript 0 and 1 refer to water and specimen, $Z = \rho c$ is the acoustic impedance. s and s_0 are the slowness (inverse of the wave-speed) of specimen and water.

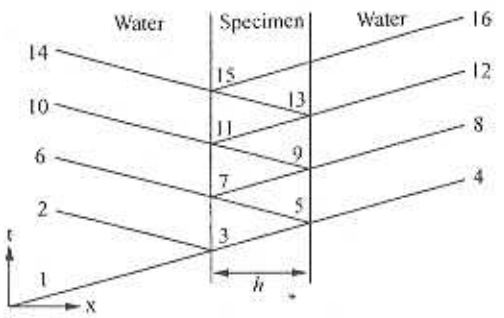

Fig. 1 Lagrangian space-time diagram of wavefront traveling through a layer

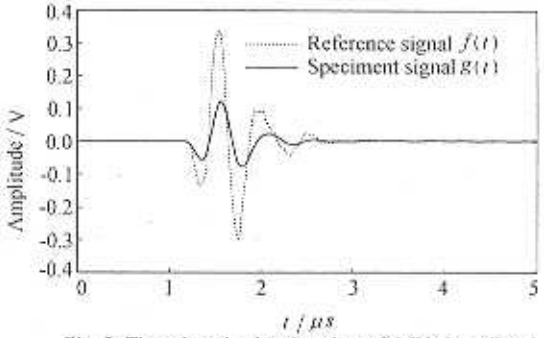

Fig. 2 Time domain signals using a 2 MHz broadband transducer. (specimen: 127 μm brass sheet)

Let $G(\omega)$ and $F(\omega)$ be the fourier transform of $g(t)$ and $f(t)$, respectively, then from Eq. (1) the transfer function of the specimen is given by

$$H(\omega) = \frac{G(\omega)}{F(\omega)} = \frac{T_{01}T_{10}e^{\mathrm{j}\,h\omega(s+s_0)}}{e^{\mathrm{j}\,2hs\,\omega} - R_{10}^2} \tag{2}$$

By introducing a dimensionless frequency $\Omega = \omega\, hs = 2\pi\, h/\lambda$, Eq. (2) may be viewed as quadratic in $\exp(-\mathrm{j}\,\Omega)$ so that Ω and, correspondingly, acoustical properties can be solved from the transfer function[13]. However, this numerical procedure was found to suffer from convergence problem in wave-speed characterization at low frequency ($h/\lambda < 0.4$), and for thickness at all frequencies. The reason for this problem has been well discussed by Kinra and Iyer *et al*[6].

One can also study the retrieve function for through-transmission. The retrieve function is the inverse of the transfer function and is given by

$$Q(\omega) = \frac{1}{H(\omega)} = \frac{1}{T_{01}T_{10}}\left[e^{-\mathrm{j}\,\omega\, h(s_0 - s)} - R_{10}^2 e^{-\mathrm{j}\,\omega\, h(s_0 + s)}\right] \tag{3}$$

Since in practice the retrieve function is measured (calculated) only at discrete frequencies, Eq. (3) is now rewritten as

$$Q(\omega_i) = \frac{1}{T_{10}T_{01}}\left[e^{-\mathrm{j}\,\omega_i\, h(s_0 - s)} - R_{10}^2 e^{-\mathrm{j}\,\omega_i\, h(s_0 + s)}\right] \tag{4}$$

It should be pointed out that only the discrete frequencies in the range of the effective bandwidth, B_d, of the transducer pairs are used. In our case, the effective bandwidth, as shown

in Fig. 3, is taken to be the frequency range in which the amplitude is great than -12 dB of the peak amplitude, i.e. 0.918 MHz - 3.463 MHz. In this frequency range, the phase was found to vary linearly with frequency.

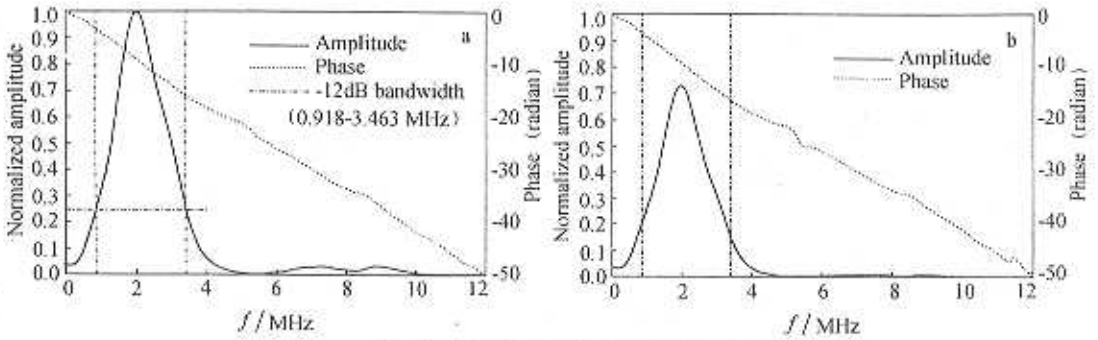

Fig. 3 Frequency domain analysis of signals
(a) Reference signal; (b) Specimen signal, (specimen: 25.4 μm brass sheet)

2.2 Error function definition

By introducing $\widetilde{Q}(\omega_i)$ as the experimentally measured retrieve function, the characterizing (inverse) problem can be posed as follows: given $\widetilde{Q}(\omega_i)$, deduce the acoustical parameter we interested. In our study, the least squares method is utilized. For any acoustical parameter, p, let $Q(\omega_i, p)$ be the theoretical retrieve function which is given by the right hand side of the Eq. (4). Therefore, a root-mean-square error function can be used to quantify the difference between the theoretical and the experimental values with p as the only variable. First, we consider the amplitude spectrum. Let $\widetilde{Q}(\omega_i)$ and $Q(\omega_i, p)$ be the amplitude spectra of measured and theoretical retrieve functions $\widetilde{Q}(\omega_i)$ and $Q(\omega_i, p)$, respectively. We now introduce an amplitude error function

$$E_{amp}(p) = \left\{ \frac{1}{N} \sum_{i=1}^{N} \left[Q_{amp}(\omega_i, p) - \widetilde{Q}_{amp}(\omega_i) \right]^2 \right\}^{1/2} \tag{5}$$

where N is the number of the discrete frequency points in effective bandwidth. The expression of $Q_{amp}(\omega_i, p)$ is given by:

$$Q_{amp}(\omega_i, p) = \frac{1}{T_{01} T_{10}} \left[1 + R_{01}^4 - 2R_{01}^2 \cos(2\omega_i sh) \right]^{1/2} \tag{6}$$

Next, we consider the phase spectrum. In the same manner as above, the expression for the phase error function, $E_{phs}(p)$, can be obtained by replacing $Q_{amp}(\omega_i, p)$ and $\widetilde{Q}_{amp}(\omega_i, p)$ by $Q_{phs}(\omega_i, p)$ and $\widetilde{Q}_{phs}(\omega_i)$ in Eq. (5), i.e.

$$E_{phs}(p) = \left\{ \frac{1}{N} \sum_{i=1}^{N} \left[Q_{phs}(\omega_i, p) - \widetilde{Q}_{phs}(\omega_i) \right]^2 \right\}^{1/2} \tag{7}$$

where the theoretical phase spectra $Q_{phs}(\omega_i, p)$ has the expression of:

$$Q_{phs}(\omega_i, p) = \omega_i h(s - s_0) + tan^{-1} \left(\frac{R_{01}^2 \sin 2\omega_i hs}{1 - R_{01}^2 \cos 2\omega_i hs} \right) \tag{8}$$

Finally, for the complex spectrum, the complex error function is defined as

$$E_{com}(p) = \left(\frac{1}{N} \sum_{i=1}^{N} \left\| Q(\omega_i, p) - \widetilde{Q}(\omega_i) \right\|^2 \right)^{1/2} \tag{9}$$

where $\| \quad \|$ denotes the modulus of a complex quantity.

The essence of our inverse scheme is that the best estimated value of p will minimize the corresponding error function. Obviously, it leads to solve a correct root of the non-linear equation in p.

3 Experimental procedures

A schematic of the through-transmission apparatus is shown in Fig. 4. A pair of accurately matched broadband water immersion longitudinal wave transducers with a center frequency of 2 MHz are used for generating and receiving the ultrasonic waves. The distance between the two transducers is adjusted to be equal to twice of the focal length with the specimen in the center. The incident short duration pulse transmits through the specimen normally and is acquired by the receiver; the received signal is then sent to a TDS-460A digital oscilloscope and digitized at a pre-set sampling rate. In order to reduce the random error, each signal is averaged 800 times before it is transferred to computer through an GPIB (IEEE-488) bus for further analysis. In our work, each signal is acquired at four sample-rates, $S_r = 2500$, 1000, 100 and 50 MHz.

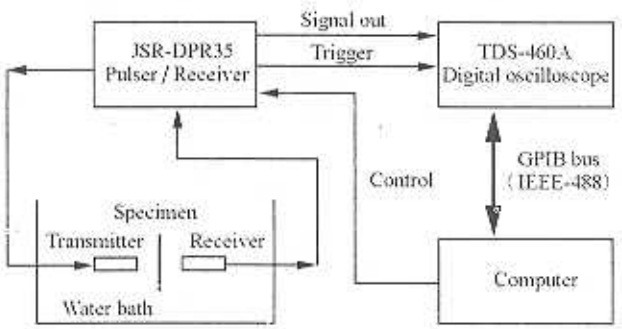

Fig. 4 Schematic of the experimental set-up

The whole data acquisition procedure consists of two independent measurements. First, with the specimen removed from the "light of sight", the reference signal, $f(t)$, is acquired. Next, with the specimen in place, the signal is acquired again, this is the transmitted signal, $g(t)$. For each specimen, the same measurement procedures are replicated 5 times.

In this work, experiments are carried out at a constant temperature, $23 \pm 0.1\ ^{\circ}C$.

4 Experimental procedures

The brass specimens of thickness ranging from 25.4 μm to 152.4 μm are tested in this study. The "true" thickness of brass plates are prescribed by vendor and verified with a micrometer, which has an error of $\pm$ 2.54 μm (0.0001 in). The nominal value of wave-speed and density for the brass sheet are, respectively, c=4.274 mm/μs and ρ = 8.4697 g/cm^3, which are known *in priori*. The numerical search is carried out over a range of about 200% of the "true" value. For example, Fig. 5 shows the error curves for different schemes (Eqs. 5, 7 and 9) against thickness, h. As expected, the three error functions all go through a well-defined minimum in the vicinity of the "true" value.

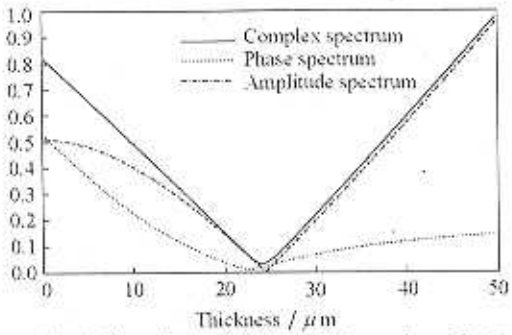

Fig. 5 Plots of error function (25.4 μm brass sheet)

The method mentioned above has been successfully employed to characterize the thickness, wave-speed and density for brass sheets and the corresponding results are listed in Table 1 – Table 3, respectively. The same procedure is applied to signals acquired at different sampling rate and some results are presented in Table 4.

Table 1 Estimation results in thickness characterization

(Specimen: brass sheets, c = 4.274 mm/μs, ρ=8.4697 g/cm^3, Sr = 2500 MHz)

Specimen thickness	Range of h/λ			Estimated using amplitude spectrum		Estimated using phase spectrum		Estimated using complex spectrum	
($\pm$ 2.54μm)	Min	Normal	Max	h_{amp}(μm)	err(%)	h_{phs}(μm)	err(%)	h_{com}(μm)	err(%)
25.40	0.00546	0.01189	0.02058	26.290	3.51	25.697	1.17	26.206	3.17
38.10	0.00764	0.01664	0.02881	37.782	-0.83	37.273	-2.17	37.874	-0.59
50.80	0.01091	0.02377	0.04116	51.627	1.63	56.079	10.39	52.136	2.63
73.66	0.01582	0.03447	0.05968	74.741	1.47	79.703	8.20	75.260	2.17
101.60	0.02183	0.04754	0.08231	101.028	-0.56	105.987	4.32	102.122	0.50
127.00	0.02728	0.05943	0.1029	126.046	-0.75	132.150	4.05	127.319	0.25
152.40	0.03274	0.07132	0.1235	150.302	-1.38	156.659	2.79	152.270	-0.08

Table 2 Estimation results in density characterization

(Specimen: brass sheets, c=4.274 mm/μs, ρ=8.4697 g/cm^3, Sr=2500 MHz)

Specimen thickness	Range of h/λ			Estimated using amplitude spectrum		Estimated using phase spectrum		Estimated using complex spectrum	
($\pm$ 2.54μm)	Min	Normal	Max	ρ_{amp}(g/cm^3)	err(%)	ρ_{phs}(g/cm^3)	err(%)	ρ_{com}(g/cm^3)	err(%)
25.40	0.00546	0.01189	0.02058	8.7629	3.46	8.5125	0.51	8.6377	1.98
38.10	0.00764	0.01664	0.02881	8.4124	0.68	8.2371	-2.75	8.3372	-1.56
50.80	0.01091	0.02377	0.04116	8.6127	1.69	7.9866	-5.70	8.4624	0.09
73.66	0.01582	0.03447	0.05968	8.5876	1.39	7.7613	-8.36	8.4624	0.09
101.60	0.02183	0.04754	0.08231	8.4124	0.68	7.6861	-9.25	8.3623	-1.27
127.00	0.02728	0.05943	0.1029	8.4124	0.68	7.4107	-12.50	8.3372	-1.56
152.40	0.03274	0.07132	0.1235	8.3623	-1.27	7.3105	-13.69	8.3122	-1.86

Table 3 Estimation results in wave-speed characterization

(Specimen: brass sheets, c=4.274 mm/μs, ρ=8.4697 g/cm^3, Sr=2500 MHz)

Specimen thickness	Range of h/λ			Estimated using amplitude spectrum		Estimated using phase spectrum		Estimated using complex spectrum	
($\pm$ 2.54μm)	Min	Normal	Max	C_{amp}(m/s)	err(%)	C_{phs}(m/s)	err(%)	C_{com}(m/s)	err(%)
25.40	0.00546	0.01189	0.02058	-	-	-	-	-	-
38.10	0.00764	0.01664	0.02881	-	-	-	-	-	-
50.80	0.01091	0.02377	0.04116	-	-	-	-	-	-
73.66	0.01582	0.03447	0.05968	-	-	-	-	-	-
101.60	0.02183	0.04754	0.08231	3935.73	-7.91	-	-	4997.50	16.9
127.00	0.02728	0.05943	0.1029	3945.74	-7.68	-	-	4546.74	6.38
152.40	0.03274	0.07132	0.1235	3895.66	-8.85	-	-	4156.09	-2.76

Table 4 Comparsion of the estimation results at different sampling rate

(Specimen: brass sheets, c=4.274 mm/μs, ρ=8.4697 g/cm^3)

Specimen Rate	Specimen thickness	Estimated using amplitude spectrum		Estimated using phase spectrum		Estimated using complex spectrum	
(MHz)	($\pm$2.54 μm)	h_{amp}(μm)	err(%)	h_{phs}(μm)	err(%)	h_{com}(μm)	err(%)
1000	25.40	26.290	3.51	25.697	1.17	26.206	3.17
100	25.40	26.290	3.51	25.697	1.17	26.206	3.17
1000	73.66	74.773	1.51	79.950	8.54	75.310	2.24
50	73.66	74.782	1.52	80.603	9.43	75.327	2.26
1000	152.40	150.237	-1.42	156.826	2.90	152.368	-0.021
100	152.40	150.237	-1.42	156.826	2.90	152.368	-0.021
50	152.40	150.237	-1.42	157.525	3.36	152.686	0.18

From Tabs. 1 and 2, it is shown that the agreement between "true" value and estimation is excellent in estimating the thickness and the density, particularly, with using amplitude and complex spectrum. The estimate error, with a few exceptions, is find to be less than 2%. Even for the thinnest specimen which has a thickness of 25.4 μm with $h/\lambda < 0.01$, the relative error is find to be about 4% which is quite acceptable considering the direct measurement error of ± 2.54 μm. However, we fail in utilizing aforementioned method to solve the inverse problem of finding the estimate of the wave-speed over the range of h/λ ratio we studied. The symbol "—" in Tab. 3 means that the corresponding estimate result is prohibitively large ($> 50\%$).

One can observed from Tab. 1 to Tab. 3 that the relative estimate error is a strong function against the change of h/λ ratio. Moreover, it also can be noticed that the estimate error is method-dependent and varies with different characterizing parameter even when processing same specimen signal (i.e. keeping the h/λ ratio as a constant). These provide the motivation for studying the reason in some detail in the next section.

5 Error analysis and discussion

There are many factors that affect the precision of the estimating results in characterizing acoustical parameter. In this section, some typical factors are examined next.

5.1 Measurement errors

The fact that the minimum of the root-mean-square residual error functions do not reach zero and, furthermore, shift from the "true" value as value show in Fig. 5 may be attributed to the presence of measurement errors in the data acquisition. It is well known that the random noise is ineluctable in the measurement. In our experiment, to improve the signal-to-noise ratio, we have the received signals coherently averaged. On the other hand, we are cognizant of the fact that the quantization distortion, which is due to the limitation of vertical resolution of the digital oscilloscope, is also an important source contributing to the measurement errors. From the comparison of Tab. 1 and Tab. 4, one can see that the almost same results are obtained. In other words, higher sampling rate does not provide extra information for a relatively smooth signal. Therefore, to choose an A/D converter with lower sampling-rate but more digital bits may be an effective way to improve the precision of our algorithm.

5.2 Sensitivity

For the inverse (characterization) problem, what we concerned is the error in estimating acoustical parameter due to the presence of measurement errors, i.e. the error propagation. Kinra *et al.* presented a detailed analysis of the through-transmission transfer function and pointed out that it is the sensitivity of the error function that plays the leading role in the propagation of errors[14]. The same conclusion has been obtained in our work using retrieve function. Instead of the normalized sensitivity defined in Kinra's papers, we have studied the sensitivities of retrieve function to three acoustical parameters theoretically.

Rewrite Eq. (3) as $Q(\omega) = Q_{amp} \cdot \exp(j\, Q_{phs})$ and let p be any acoustical parameter we interested. We now introduce a complex value sensitivity of $Q(\omega)$

$$S(Q,p) = p\frac{\partial Q}{\partial p} \tag{10}$$

which denotes the change in $Q(\omega)$ due to one unit normalized change in p. Similarly, the sensitivity of magnitude and phase to p are defined respectively as

$$\begin{aligned} S(Q_{amp},p) &= p\frac{\partial Q_{amp}}{\partial p} \\ S(Q_{phs},p) &= p\frac{\partial Q_{phs}}{\partial p} \\ S(Q,p) &= [S(Q_{amp},p) + j\, Q_{amp} S(Q_{phs},p)]\exp(j\, Q_{phs}) \end{aligned} \tag{11}$$

Let $e[\widetilde{Q}(\omega_i)]$ be the absolute error in measuring $Q(\omega)$. Then, $\widetilde{Q}(\omega_i) = Q(\omega_i,\hat{p}) + e[\widetilde{Q}(\omega_i)]$, where $\hat{p}$ denotes the nominal value of characterizing parameter p. Because of the presence of measurement errors, it will lead to an absolute estimate error, $e(p)$, between the estimation, p_e, and the true value, $\hat{p}$. Now, we expand the $Q(\omega_i, p_e)$ in a Taylor-series about $\hat{p}$ and retain only the linear terms in $e(p)$:

$$Q(\omega_i,p_e) = Q(\omega_i,\hat{p}) + e(p)\frac{\partial Q(\omega_i,\hat{p})}{\partial \hat{p}} = Q(\omega_i,\hat{p})[1 + err(p)S_n(Q,\hat{p})] \tag{12}$$

where $err(p) = e(p)/\hat{p}$ is the relative error in estimating and $S_n(Q,p) = S(Q,p)/Q(\omega_i,p)$ is defined as the normalized sensitivity of retrieve function which indicates the normalized change in $Q(\omega)$. Furthermore, we assume that $S_n(Q,p_e) \approx S_n(Q,\hat{p})$ then, through a lengthy calculation, it can be shown that:

$$err(p) = \frac{\sum_{i=1}^{N}[e(Q_{amp})S(Q_{amp},\hat{p}) + e(Q_{phs})S(Q_{phs},\hat{p})(Q_{amp})^2]}{\sum_{j=1}^{N}\|S(Q,\hat{p})\|^2} \tag{13}$$

where $e(Q_{amp}$ and $e(Q_{phs})$ indicate the absolute error in measuring the amplitude and phase spectrum respectively. It is clear that the relative estimate error has a strong relation with the sensitivity of the error function provided that the measurement error is same, such as the same specimen signal been processed. When the sensitivity is low, a small error in measurement can lead to a large error in estimating and vice versa. In the same way, when we only treat the amplitude or phase spectrum, relationship between estimate errors and error function similar to Eq. (13) can also be deduced.

From Eqs. (6), (8) and (11), we can get various sensitivity functions against each acoustical parameter, the analytical expressions are as follows

$$S(Q_{amp},h) = \frac{2R_{10}^2\omega\, hs\sin(2\,\omega\, hs)}{(1-R_{10}^2)[1+R_{10}^4 - 2R_{10}^2\cos(2\,\omega\, hs)]^{1/2}} \tag{14}$$

$$S(Q_{phs},h)=\omega h(s-s_0)+\frac{2R_{10}^2\omega hs[\cos(2\omega hs)-R_{10}^2]}{1+R_{10}^4-2R_{10}^2\cos(2\omega hs)} \tag{15}$$

$$S(Q_{amp},s)=\frac{2R_{10}^2\omega hs\sin(2\omega hs)-R_{10}(1+R_{10}^2)[1-\cos(2\omega hs)]}{(1-R_{10}^2)[1+R_{10}^4-2R_{10}^2\cos(2\omega hs)]^{1/2}} \tag{16}$$

$$S(Q_{phs},h)=\omega hs+\frac{2R_{10}^2\omega hs[\cos(2\omega hs)-R_{10}^2]}{1+R_{10}^4-2R_{10}^2[\cos(2\omega hs)} \tag{17}$$

$$S(Q_{amp},d)=\frac{R_{10}(1+R_{10}^2)[1-\cos(2\omega hs)]}{(1-R_{10}^2)[1+R_{10}^4-2R_{10}^2\cos(2\omega hs)]^{1/2}} \tag{18}$$

$$S(Q_{phs},d)=\frac{R_{10}(1-R_{10}^2)\sin(2\omega hs)}{1+R_{10}^4-2R_{10}^2\cos(2\omega hs)} \tag{19}$$

One can observed that the sensitivity of error function is both material dependent and frequency dependent. The sensitivity curves as a frequency-dependent function of h, ρ and s for brass plate over the range of h/λ ratio we studied ($h/\lambda \leq 0.1$) are plotted in Figs. 6, 7 and 8, respectively.

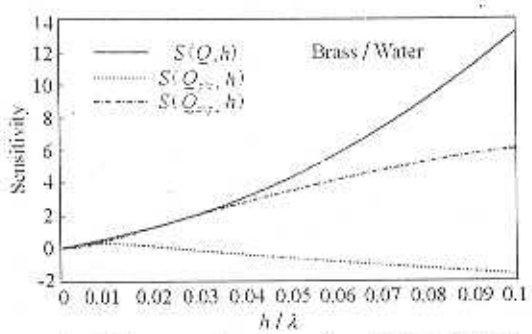

Fig. 6 Frequency dependence of sensitivity of retrieve function against the change of thickness

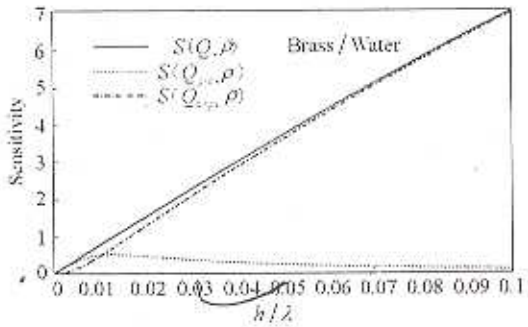

Fig. 7 Frequency dependence of sensitivity of retrieve function against the change of density

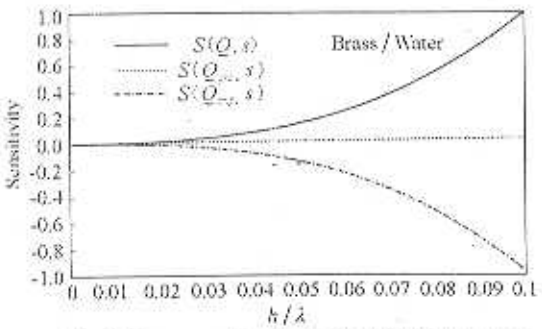

Fig. 8 Frequency dependence of sensitivity of retrieve function against the change of wave-speed

Using frequency-depend sensitivity curves illustrated in Figs. 6, 7 and 8, we can give a reasonable explication for the relative estimate error varying from the difference of h/λ ratio as well as error function employed. If we notice the fact that the sensitivity curve $S(Q_{phs},h)$ crosses zero at the vicinity of $h/\lambda = 2\%$, it is understandable that the corresponding estimation

errors of thickness using phase spectrum become large. Consistent with the sensitivity curve $S(Q_{phs}, d)$ shown in Fig. 7, it can be observed in Tab. 2 that the relative estimate error increases as h/λ increases. Furthermore, the reason for our inverse scheme failures in estimating wave-speed can be attributed to the fact that the algorithm has very low sensitivity against the change of wave-speed, which are demonstrated in Fig. 8.

5.3 Attenuation

According to the aforementioned analysis and sensitivity curve (Q_{amp}, h) shown in Fig. 6, it might be a rational expection that the relative estimate error using amplitude spectrum should decrease as the thickness of specimen increases. However, it is observed from Tab. 1 that the relative error is rather large in measurement the specimen of 152.4 μm. Similar phenomena can also be found in references[12,14]. The reason for this is due to attenuation. In Eqs. (1) to (3) we have ignored the attenuation for simplicity so that the received signal was considered to maintain the original form of the incident wave except the reduction of amplitude due to acoustic mismatch. The estimate deviation induced by the neglect of attenuation is material dependent and will become worse as the thicker specimen. On the other hand, the phase spectrum is found to be insensitive to attenuation. This is not at all surprising in view of the fact that the phase of the longitudinal wave carries no information of the amplitude in an unbounded medium. Therefore, the phase spectrum should be more dependable in the thickness characterization.

6 Conclusion

Undoubtedly, it has theoretical and engineering importance for non-destructive evaluation of the acoustical parameters of ultra-thin specimen using low frequency ultrasound. The frequency domain through-transmission retrieve function scheme has been utilized successfully in estimating acoustical parameters for ultra-thin brass sheets with $0.005 < h/\lambda < 0.1$ in this paper. Through the theoretical and experimental study, some conclusions are presented as follow

1. It has been found that the retrieve function method works excellent in thickness and density characterizing with estimate error less than 4%.

2. The estimate errors come from the presence of measurement errors in data acquisition as well as the theory assumption deviation. Eq. (13) quantifies the significance of sensitivity in the propagation of errors. Clearly, when the sensitivity is low, a small error in measurement can lead to a large error in estimating and vice versa.

3. In the case of wave-speed characterization, it has been shown that our inverse algorithm has very low sensitivity against the change of wave-speed over the range of h/λ ratio we studied in this paper and, correspondingly, the estimate errors are prohibitively large.

4. Compared to the transfer function method, the retrieve function method not only has better sensitivity but also can be readily extended to characterize multi-layered specimen. For the subject of layered media characterizing, we will report in another paper.

References

[1] Papadakis E P. Ultrasonic velocity and attenuation: Measurement methods with scientific and industrial applications. In: Mason W N eds. Physical Acoustics Principles and Methods (vol. 12), New York: Academic Press, 1976: 277–374

[2] Krautkramer J, Krautkramer M. Ultrasonic testing of materials. 4th fully revised edition, Spring Verlag, 1990

[3] Light G M, Singh G P, McDaniel F D. Ultrasound and X-ray fluorescence measurement of the thickness of metal foils. *Materials Evaluation*, 1989; **47**: 322–330

[4] Mcksimin H L. Pulse superposition method for measuring the velocity of sound in solids, *J. Acoust. Soc. Am.*, 1961; **33**(1): 12–16

[5] Chang F H, Couchman J C, Yee B G W. Ultrasonic resonance measurements of sound velocity in thin composite laminates. 1974; **8**(10): 356–363

[6] Kinra V K, Iyer V R. Ultrasonic measurement of the thickness, phase velocity, density or attenuation of a thin-viscoelastic plate. Part I: the forward problem. *ultrasonics*, 1995; **33**(2): 95–110

[7] Kinra V K, Iyer V R. On the use of phase spectra for ultrasonic NDE. Proceeding of the 1990 SEM spring conference on experimental mechanics, Albuquerque New Mexico, 1990: 478–485

[8] Pialucha, Guyott C C H, Cawley P. An amplitude spectrum method for the measurement of phase velocity. *Ultrasonics*, 1989; **27**: 332–339

[9] WAN Mingxi, Jiang B, CAO Wenwu. Direct measurement of ultrasonic velocity of thin elastic layers. *J. Acoust. Soc. Am.*, 1997; **101**(1): 626–628

[10] Kinra V K, Zhu C. Time-domain ultrasonic NDE of the wave velocity of a sub-half-wavelength elastic layer. *J. of Testing and Evaluation*, 1993; **21**(1): 29–35

[11] Zhu C, Kinra V K. Time-domain ultrasonic measurement of the thickness of a sub-half-wavelength elastic layer. *J. of Testing and Evaluation*, 1992; **20**(4): 265–274

[12] Zhu C, Kinra V K. A new technique for time-domain ultrasonic NDE of thin plates, *J. of nondestructive evaluation*, 1993; **12**(2): 121–131

[13] Kinra V K, Dayal V. A new technique for ultrasonic-nondestructive evaluation of thin specimens. *J. Exp. Mech.*, 1988; **28**(3): 288–297

[14] Kinra V K, Iyer V R. Ultrasonic measurement of the thickness, phase velocity, density or attenuation of a thin-viscoelastic plate. Part II: the inverse problem. *ultrasonics*, 1995; **33**(2): 111–122

[15] Iyer V R, Kinra V K. Frequency-domain ultrasonic measurement of the thickness of a sub-half-wavelength adhesive layer. Proceeding of the 1991 SEM spring conference on experimental mechanics, Milwaukee Wisconsin, 1991: 668–675

[16] Hanneman S, Kinra V K. A new technique for ultrasonic-nondestructive evaluation of adhesive joints: Part I. Theory. *J. Exp. Mech.*, 1992, **32**(4): 323–331

[17] Zhu C, Kinra V K. Ultrasonic nondestructive evaluation of thin (sub-wavelength) coatings. *J. Acoust. Soc. Am.*, 1993; **93**(5): 2454–2467

[18] Kinra V K, Jaminet P, Zhu C *et al.* Ultrasonic nondestructive evaluation of a three-layered medium. *Materials evaluation*, 1994; (8): 948–953